In-situ SEM/EBSD observation of hydrogen-assisted cracking of ultra-fine grained austenite

Arnaud Macadre[1*], Toshihiro Tsuchiyama[1,2], Setsuo Takaki[1,2]

[1] International Institute for Carbon-Neutral Energy Research (I²CNER), Kyushu University, Japan
[2] Department of Materials Science & Engineering, Kyushu University, Japan

Abstract: Hydrogen infrastructure requires steels that are not affected adversely by hydrogen. For the sustainability of such an infrastructure, strength, cost and hydrogen compatibility need to be brought together. One way is grain refinement. With ultra-fine grained austenite, the yield stress is 600 MPa (with 1 μm grains). To observe how the fracture mechanism evolves, notched tensile specimens were prepared, with three grain sizes, increasing from 1 μm to 21 μm. Hydrogen was charged thermally in the specimens, and tensile tests were conducted within an SEM chamber with an EBSD camera. The tensile tests were interrupted several times before and after yielding, up to fracture, to observe the evolution of microstructure and the cracking path. Fracture surface observation was also conducted to supplement surface analysis. It was found that regardless of grain size, intergranular fracture occurred. Ultra-fine grains however retained a ductile fracture behaviour, while the coarsest grains failed in a complete brittle manner.

1. INTRODUCTION

Stable austenitic stainless steels, such as SUS316, SUS316L or SUH660, are said to be relatively resistant to the adverse effects of hydrogen, due to their high nickel content and associated austenitic phase stability. However, their strength is either too low (SUS316), requiring large quantities of steel to ensure safety, or high enough, but with a very high base cost (SUH660). In either case, the final cost makes it prohibitive to deploy stable austenitic stainless steels on a large scale for hydrogen infrastructure. We propose an ultra-grain-refinement process on metastable austenite as a means of keeping costs low while increasing strength of the alloy. Metastable stainless steels however are said to be much more prone to the so-called hydrogen embrittlement (HE), or at least severe hydrogen-induced reduction of ductility. Furthermore, ultra-fine grains usually require specific equipment, such as ECAP (Equal Channel Angular Extrusion) or HPT (High Pressure Torsion). Here, cold-rolling and annealing are used for a specific chemical composition of metastable austenitic stainless steel, which allows grain refinement. This study is based on tensile testing with analysis of both fracture surface and microstructure evolution in the presence of solute hydrogen.

2. MATERIAL AND METHODOLOGY

The steel used in this study is Fe-16Cr-10Ni [1]. This composition is very suitable to control the grain size of austenite down to 1 μm by conventional thermo-mechanical treatment, *i.e.* rolling and annealing. Cold-rolling to a 90% thickness reduction resulted in more than 90% of the material transforming into α'-martensite. This is followed by annealing, where the conditions were 10 min. at 923 K, 10 min. at 1023 K or 30 min. at 1173 K, followed by air cooling. The material was fully austenitic after annealing. The grain sizes were 1, 5.8 and 21 μm after annealing at 923 K, 1023 K and 1173 K respectfully. Figure 1 shows the corresponding EBSD maps. It is to be noted that annealing twins are present in all three materials and that the twin boundaries appear to be incoherent. The naming convention for each grain size is: UFG16-10 (1 μm), MG16-10 (5.8 μm), CG16-10 (21 μm).

Tensile specimens with a notch were cut out by electrical discharge machining (EDM) (Fig. 2) and were all polished to a buff, followed by an electro-chemical polishing bath in phosphoric and chromic acid for 20 min. to remove surface damage and EDM damage. Finally the notched specimens were further prepared with colloidal silica. The stress concentration factor at the root of the notch was calculated to be $K_t = 5.6$.

---

[*] Corresponding author. E-mail: macadre@i2cner.kyushu-u.a.cjp, telephone: +81 (0)92 802 6693.

Before tensile testing, the specimens were exposed to 100 MPa high pressure hydrogen gas for 72 hours at 543 K. The notched tensile specimens were tested within the SEM chamber, in vacuum, with a crosshead speed of 5.0 μm.min^{-1}. Lastly, the EBSD step size was 0.5 μm for 21 μm grains, 0.1 μm for 5.8 μm grains and 0.02 μm for 1 μm grains.

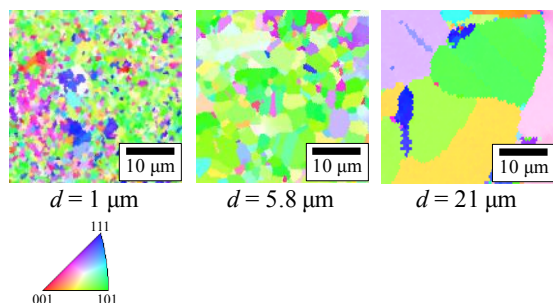d = 1 μm d = 5.8 μm d = 21 μm

Fig. 1: EBSDS inverse pole figure maps (IPF) for each grain size
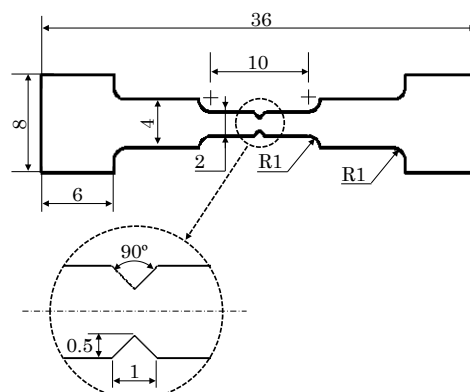

Fig. 2: Notched tensile specimen for testing in the SEM chamber

3. RESULTS AND DISCUSSION
3.1. Results

Uncharged notched Fe-16Cr-10Ni specimens were previously tested but, due to the high ductility, failure could not be reached and surface deformation prevented any significant analysis. Therefore, only hydrogen-charged samples are presented in this report. After hydrogen charging, the hydrogen content was evaluated with thermal desorption spectroscopy, with a heating rate of 0.33 K.s^{-1} and up to a maximum temperature of 1073 K. The hydrogen content C_H was evaluated to be C_H = 70.1 wppm.

The stress-strain curves at the notch root for the interrupted in-situ tensile testing are shown in Figure 3, taking the stress concentration into account. Each drop of the stress-strain curves corresponds to an EBSD measurement. For reasons still unclear, the stress of UFG16-10 dropped some time after yielding. It is interesting to note that both UG16-10 and MG16-10 show a smooth decrease in stress before fracture while CG16-10 appeared to experience a sudden drop in stress before fracture, indicating a possible difference between ductile fracture (UFG16-10 and MG16-10) and a more brittle fracture (CG16-10).

Direct observation of the notch root in all three materials showed that UFG16-10 and MG16-10 broke suddenly after necking, as in common ductile fracture after necking, while in CG16-10, small cracks originated at the notch root, coalesced and propagated onto the specimen surface, leading to fracture. Both behaviours correspond to the stress-strain curve data and Figure 4 shows SEM micrographs taken soon after cracking initiated. EBSD phase maps are shown in Figure 5, showing the microstructure previous to fracture. Finally, Figure 6 shows details of the fracture surfaces for each hydrogen-charged material. UFG16-10 and MG16-10 show tearing at grain boundaries as well as void formation around inclusions. The facets observed in UFG16-10 and MG16-10 show plastic deformation. Conversely, no such void formation around inclusions could be observed in CG16-10. Intergranular fracture was also observed and slip lines were clearly observed on facets, with secondary cracking initiating at slip lines intersections. In all samples, the intergranular fracture showed clear slip lines, meaning that even with a large degree of embrittlement, failure was ultimately ductile. Furthermore the phase maps in Figure 5 show that the material underwent serious martensitic transformation at the notch root prior to failure.

3.2. Discussion

It has been previously stated by several research groups [2-5] that martensitic transformation is not the cause for embrittlement in metastable austenitic stainless steels. Rather, twin boundaries present a weak point in the presence of hydrogen, and even when martensitic transformation takes place in the presence of solute hydrogen, cracking does not occur in the freshly made martensite-austenite boundary [4].
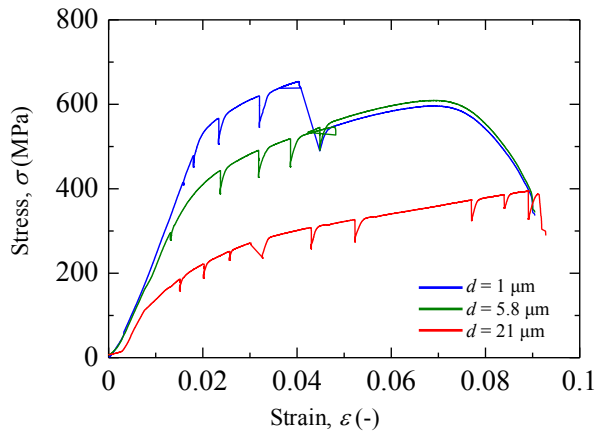
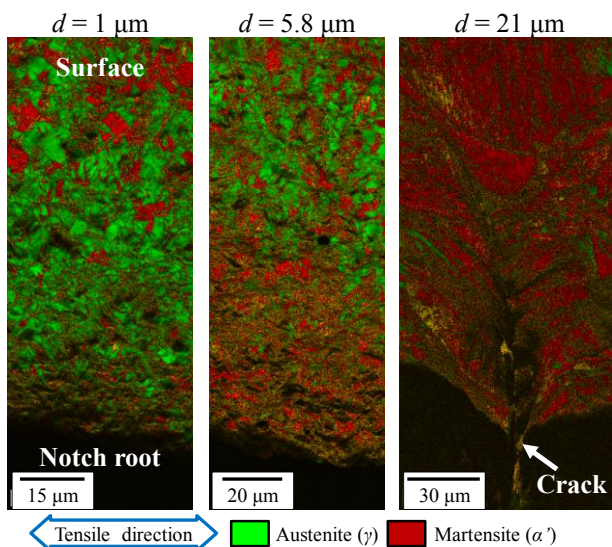Fig. 3: Stress-strain curve for the hydrogen-charged notched tensile specimens

Fig. 5: Phase maps for each grain size, prior to failure. Note that only the coarse grains had a propagating crack.
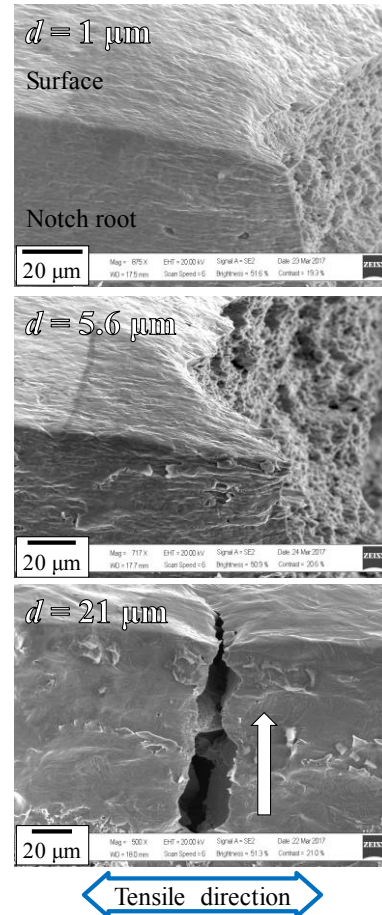

Fig. 4: SEM micrographs at the notch root just after crack initiation. The white arrow indicates a propagating crack in CG16-10. Note that no such cracking could be observed in the finer grains.

Conversely, Mine *et al.* [6, 7] explained how martensitic transformation could be linked to increased shear deformation, which would then link to fracture. The hydrogen solubility in α'-martensite is about two orders of magnitude lower than in austenite, but the hydrogen diffusivity in α'-martensite is much higher than in austenite. Austenite-to-martensite transformation would thus lead to a large amount of excess hydrogen in the freshly formed martensite, this hydrogen can in turn diffuse into the neighbouring austenite, but, due to the low hydrogen diffusivity of austenite, hydrogen would remain in the vicinity of the freshly formed austenite-martensite interface. The accumulated hydrogen would then cause cracking. In the present study, it is however clear that virtually no austenite remains at the notch root. Furthermore, in the CG16-10 material, a crack is present in an almost purely martensitic area, with no evidence of austenite around the crack. This crack was also the starting point for the ultimate failure of the specimen. It has been shown that hydrogen does enhance slip planarity [8, 9] and that hydrogen greatly enhances dislocation activity [10, 11]. In the present work, it appears martensitic transformation preceded any major failure. Furthermore, no austenite-martensite interfaces could be observed. While it is possible that such interfaces were a starting point for cracking, the general weakening of grain boundaries is likely the main reason failure occurred in all grain sizes. Since the smaller grains, UFG16-10 and MG16-10, failed in a more ductile manner, it is deemed that the refined grain size led to a lower dislocation activity than in CG16-10. The increased dislocation activity, along with hydrogen transport by dislocation to grain boundaries

and other obstacles, such as inclusions, however, led to a large amount of brittle features on all the fracture surfaces.
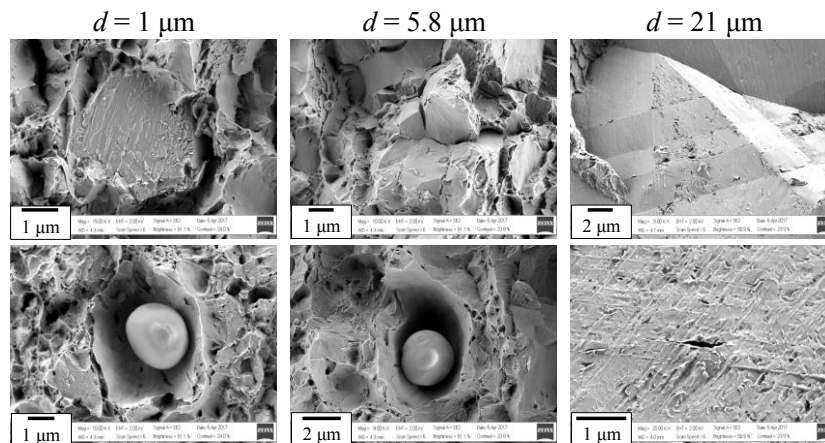

Fig. 6: Examples of fracture surfaces for each grain size.

4. CONCLUDING REMARKS

After gaseous hydrogen charging of a metastable austenitic stainless steel with different grain sizes, tensile tests inside an SEM with notched specimens were conducted. The results and conclusions are the following:

1. With 70 wppm solute hydrogen, intergranular failure was present for all grain sizes, but in all cases the intergranular fracture surfaces showed clear plasticity and slip activity, meaning that ultimately the failure was ductile in nature.

2. There was a clear difference in behaviour between the coarse grained material and the finer grained materials. Finer grained materials displayed void formation around inclusions. The coarse grained material displayed very brittle behaviour without significant void formation and large amounts of secondary cracking along slip bands and at slip intersections.

3. Finally, the failure mechanism is believed to be a combination of high dislocation activity along with stress concentrations at either inclusions or slip bands intersections. Such stress concentrators allow for high dislocation activity. Hydrogen-carrying dislocations will affect the character of interfaces, by increasing damage and bringing further hydrogen into the interfaces. This leads to intergranular failure.

REFERENCES

[1] K. Tomimura, S. Takaki, S. Tanimoto, Y. Tokunaga: ISIJ International, 31 (1991), 721–727.
[2] A. W. Thompson: Materials Science and Engineering, 14 (1974), 253–264.
[3] G. R. Caskey, Jr.: Scripta Metallurgica, 11 (1977), 1077–1083.
[4] C. San Marchi, N. Y. C. Yang, T. J. Headley, J. Michael: Proceedings of the 18th European Conference on Fracture (ECF18) (2010)
[5] M. Hatano, M. Fujinami, K. Arai, H. Fujii, M. Nagumo: Acta Materialia, 67 (2014), 342–353.
[6] Y. Mine, D. Haraguchi, T. Ideguchi, N. Horita, Z. Horita, K. Takashima: ISIJ International, 56 (2016), 1083–1090.
[7] Y. Mine, N. Horita, Z. Horita, K. Takashima: International Journal of Hydrogen Energy, 42 (2017), 15415–15425.
[8] D. P. Abraham, C. J. Altstetter: Metallurgical and Materials Transactions A, 26 (1995), 2859–2871.
[9] K. A. Nibur, D. F. Bahr, B. P. Somerday: Acta Materialia, 54 (2006), 2677–2684.
[10] I. Aubert, J-M. Olive, N. Saintier: Materials Science and Engineering A, 527 (2010), 5858–5866.
[11] I. M. Robertson: Engineering Fracture Mechanics, 68 (2001), 671–692.